https://doi.org/10.5194/egusphere-2025-6356
Preprint. Discussion started: 30 December 2025

Leaching Behavior of Steelmaking Slag Fertilizer under Repeated Wetting and Drying Conditions Simulating Upland Soil

Takayuki Iwama[1], Shohei Koizumi[2], Megumi Obara[1], Shigeru Ueda[1]

[1] Institute of Multidisciplinary Research for Advanced Materials, Tohoku University, 2-1-1, Katahira, Aoba-ku, Sendai, 980-8577 Japan
[2] Advanced Technology Research Laboratories, Nippon Steel, 20-1, Shintomi, Futtsu, 293-8511, Japan

Correspondence to: Takayuki Iwama (takayuki.iwama.a6@tohoku.ac.jp)

Abstract. To determine how steelmaking slag dissolves and modulates soil acidity and exchangeable cations under upland-like repeated wetting–drying conditions, we conducted a soil-column experiment. Specifically, we aimed to identify the Ca-supplying phases responsible for pH correction, evaluate their persistence during extended leaching, and define the layer-scale reach of the effect to inform application planning (rate, placement, and maintenance). Soil columns incorporating discrete slag-amended layers were prepared together with unamended controls. A repeated wetting–drying leaching test was run up to 24 weeks; after termination, each column was sampled by layer, and soil pH and exchangeable CaO were measured. Additionally, surfaces and cross-sections of slag particles embedded in the columns were observed to identify dissolving phases and secondary precipitates. In the control columns, soil pH remained in the acidic range (4.8–5.5), whereas slag-amended layers maintained pH 6.0–6.5 for 24 weeks in the test columns. Adjacent unamended layers in the test columns showed no detectable change, indicating that the effect was confined to the amended layers. Exchangeable CaO increased in soils mixed with slag. Microstructural observations revealed alteration and dissolution of free lime (f-CaO) and dicalcium silicate ($2CaO \cdot SiO_2$), with $CaCO_3$ precipitates on particle surfaces. These Ca-supplying phases persisted after 24 weeks of leaching. Sustained Ca release from f-CaO and $2CaO \cdot SiO_2$, together with $CaCO_3$ precipitation, produced localized, durable pH correction in slag-amended layers while leaving adjacent layers unchanged. The defined reach and persistence provide a mechanistic basis for application planning in acidic upland soils – informing rate, placement within the profile, and maintenance intervals.

1 Introduction

Steelmaking slag is a by-product generated during steel production. It is produced in the process of converting pig iron, which is obtained by reducing iron ore in a blast furnace, into tough steel by removing impurities such as carbon, phosphorus, and sulfur. The properties of steelmaking slag vary depending on the steelworks and the type of steel being produced; however, its main components typically include lime (CaO), silica (SiO_2), iron oxide (FeO_x), magnesia (MgO), manganese oxide (MnO), and phosphate (P_2O_5), all of which are beneficial to plant growth (Nippon Slag Association 2015). Steelmaking slag is primarily used as a fertilizer material in paddy fields. It supplies silica to rice plants, which strengthens their resistance to lodging, high temperatures, and pests (Ahire et al. 2021; Verma et al. 2024). It also helps suppress reductive conditions in

https://doi.org/10.5194/egusphere-2025-6356
Preprint. Discussion started: 30 December 2025

paddy soils by replenishing iron and manganese that leach out, thereby preventing "aki-ochi" – a decline in rice yield caused by hydrogen sulfide generation (Shiratori 2024). In addition, controlling methane emissions, which are released as a result of reduction processes occurring in paddy soils (Appelo and Postma 2004), has become an important goal for sustainable rice farming, and slag use is expected to contribute to the reduction of greenhouse gas emissions (Ito 2015; Inubushi et al. 2018; Inubushi 2021; Yamamoto and Morii 2020).

Steelmaking slag fertilizers are also beneficial in upland fields. When applied for soil pH correction, it can raise soil pH to weakly alkaline levels without leading to growth inhibition associated with micronutrient deficiencies. Soil pH has been raised to around 7.5 as a means of suppressing soil-borne diseases such as clubroot in Brassica crops and bacterial wilt in tomatoes (National Agriculture and Food Research Organization 2015). Moreover, the effect of steelmaking slag fertilizer in improving soil pH has been reported to last longer than that of conventional liming materials such as calcium carbonate (Goto 2016), making it possible to maintain the effect over an extended period with a single application.

Steelmaking slag also contains phosphate, one of the three essential nutrients for stable food production. Although the P_2O_5 content in slag ranges from 2 to 10 mass% (Matsubae–Yokoyama et al. 2009) and is lower than that in conventional phosphate fertilizers such as fused phosphate or superphosphate (Food and Agriculture Materials Inspection Center 2024), Japan, which is one of the world's largest steel producers, generates approximately 12 million tons of steelmaking slag annually (Nippon Slag Association 2024). Assuming a P_2O_5 concentration of 3.5 mass%, the total phosphorus contained in slag corresponds to Japan's annual phosphorus imports (JOGMEC 2021). In recent years, the importance of exploring underutilized domestic resources that contain N, P, and K has increasingly been recognized for the sustainability and stability of agriculture, further enhancing the value of steelmaking slag as a fertilizer material.

To meet this growing demand, it is necessary to clarify the amount and rate of nutrient release from steelmaking slag fertilizers into soil, which is essential for integrating slag into broader fertilization strategies. Various leaching tests have been conducted in paddy environments, mainly focusing on the supply of silica (Gao et al. 2015; Ito 2022; Maruoka et al. 2015; Okubo et al. 2015). For example, it has been reported that the amount of silica actually absorbed by rice plants is better predicted not by total silicon content or the amount extractable with 0.5 mol/L HCl, but rather by the plant-available silica extractable in near-neutral solutions such as tris buffer (Furuzono et al. 2022). Moreover, studies involving slag embedded in actual paddy soils and analyzed via cross-sectional observation (Ito et al. 2015; Ito 2022) have shown that $2CaO{\cdot}SiO_2$ is the main source of plant-available silica in weakly acidic to neutral conditions, and that there are significant differences in silica supply ability among various silicate minerals in slag.

Studies on the use of steelmaking slag fertilizer in upland fields have mainly focused on how changes in soil pH caused by slag application affect crop yield, nutrient uptake, or the incidence of soil-borne diseases (Deus et al. 2020; Iwadate 2017; Murakami and Goto 2006; Sinegovskaya et al. 2020). However, there is limited research on the specific dissolution behavior of slag in upland soils. Unlike paddy soils, which are saturated with water and exist under reducing conditions due to limited oxygen supply (Maruoka et al. 2015), upland soils experience alternating wet and dry cycles and are exposed to atmospheric oxygen, resulting in oxidative conditions. These environmental differences suggest that the dissolution behavior of slag

https://doi.org/10.5194/egusphere-2025-6356
Preprint. Discussion started: 30 December 2025

fertilizer would differ significantly between paddy and upland conditions. In upland farming, the primary expected benefit of steelmaking slag fertilizer is its ability to increase soil pH, attributed to its alkaline components, such as Ca^{2+} and Mg^{2+}. However, the alkaline components in slag exist in various mineral forms, including not only CaO, $Ca(OH)_2$, and $CaCO_3$ as found in typical liming agents, but also $2CaO{\cdot}SiO_2$, $2CaO{\cdot}Fe_2O_3$, $Ca_2MgSi_2O_7$, and $Ca_2Al_2SiO_7$ (Gao et al. 2015; Ito et al. 2015). Understanding how each of these mineral phases dissolves is crucial for designing effective fertilizer application strategies aimed at improving soil pH. In addition, understanding how phosphorus, iron, manganese, and other micronutrients dissolve is important for realizing the full potential of steelmaking slag as a fertilizer. Therefore, this study investigates how steelmaking slag fertilizer dissolves under conditions simulating upland field environments, and evaluates its effects on soil pH, exchangeable cations, and plant-available phosphorus. The same observational scheme can provide a common basis when comparing fertilizer behavior across products under identical hydrologic forcing.

2 Experimental

2.1 Samples

The soil used in this study was Andosol, which accounts for approximately 45.1% of Japan's land area and is widely used in agricultural fields (Saigusa and Matsuyama 1998). The test soil had a gravimetric water content of 41% on a dry weight basis. A commercially available fertilizer was used, which is produced by pulverizing steelmaking slag. The chemical composition of the slag fertilizer is shown in Table 1. The elemental composition was determined by digesting the slag sample in a mixture of hydrochloric acid, nitric acid, and hydrofluoric acid, followed by analysis of the solution using inductively coupled plasma–atomic emission spectroscopy (ICP–AES). The concentrations of each element were converted to their corresponding oxide forms (Fe was expressed as FeO). The category labeled "Others" is presumed to represent H_2O and CO_2 that reacted with the slag fertilizer.

Table 1 Chemical composition of steelmaking slag fertilizer.

CaO	SiO_2	FeO	MgO	MnO	Al_2O_3	P_2O_5	Others
40.9	10.7	21.4	6.6	2.1	3.0	1.8	13.5

The X-ray diffraction (XRD) pattern of the slag fertilizer is shown in Fig. 1. Diffraction peaks corresponding to $Ca(OH)_2$, $CaCO_3$, $2CaO{\cdot}SiO_2$ (C_2S), $3CaO{\cdot}SiO_2$ (C_3S), MgO–FeO solid solution (MF), and $2CaO{\cdot}Fe_2O_3$ (C_2F) were identified, indicating that the slag fertilizer consists of multiple mineral phases. A broad halo pattern was also observed between 25° and 40°, suggesting the presence of an amorphous glass phase. These mineral phases are commonly found in typical steelmaking

https://doi.org/10.5194/egusphere-2025-6356
Preprint. Discussion started: 30 December 2025

slag (Gao et al. 2015; Gu et al. 2025; Li et al. 2024; Matsui 2020), and the slag fertilizer used in this study is not a specialized product, but one derived from general blast furnace–basic oxygen furnace (BF–BOF) process slag.

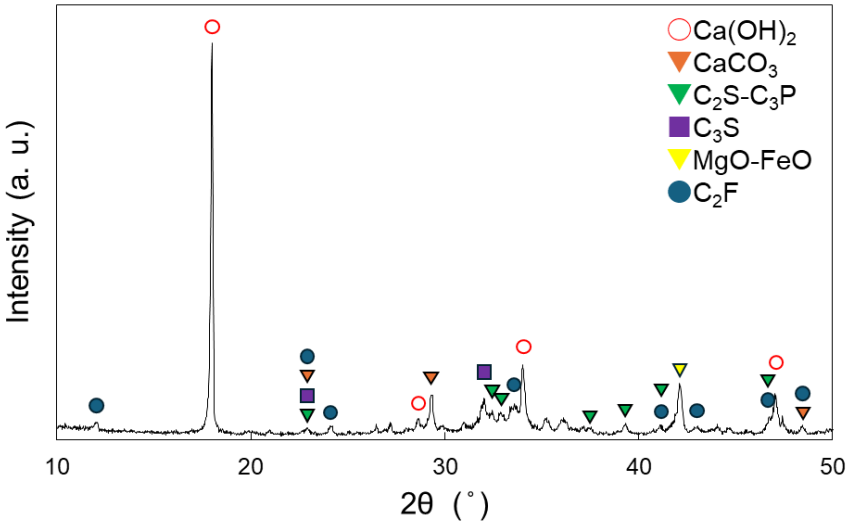

Fig. 1 XRD pattern of slag fertilizer.

2.2 Experimental Apparatus

A schematic of the experimental apparatus is shown in Fig. 2. To simulate upland soil conditions, including evaporation from the soil surface and downward water infiltration, a soil column apparatus was constructed using the following procedure: A rigid polyvinyl chloride (PVC) cylinder (inner diameter: 52 mm; length: 500 mm) was used. One end of the cylinder was sealed with a silicone rubber stopper containing a 10 mm diameter hole at its center. A vinyl hose (outer diameter: 10 mm; inner diameter: 8 mm; length: 50 mm) was inserted into the hole to allow water drainage. A piece of gauze (diameter: 40 mm) was placed over the rubber stopper from the open end of the column to prevent soil loss. To build the base soil layers, 85 g of the test soil was packed into the column while tapping to ensure uniform compaction, forming a layer approximately 5 cm thick. A plastic mesh (diameter: 52 mm) was then placed on top of the soil. This process was repeated two more times to build a total of three soil layers, with plastic mesh inserted between each layer to separate them for post-experiment sampling. Next, three layers of a soil–slag mixture were prepared, each consisting of 85 g of soil and 1 g of slag fertilizer powder that passed through a 212-micrometer sieve (hereafter referred to as the soil–slag mixture). Each mixture layer was packed into the column using the same tapping method, with a plastic mesh placed between each. In the middle of the three mixture layers, a resin-embedded slag fertilizer sample (diameter: 25 mm; thickness: 10 mm) containing a mirror-polished slag particle (maximum size: 1.7 mm (Food and Agriculture Materials Inspection Center 2024) was installed. The polished surface was oriented perpendicular to the bottom of the column, allowing surface observations before and after the test. Finally, with all three soil–

https://doi.org/10.5194/egusphere-2025-6356
Preprint. Discussion started: 30 December 2025

slag mixture layers built, the construction of the soil column leaching test apparatus and test samples (test group) was completed. As a control, columns containing six layers of soil only – without slag fertilizer and without embedded resin samples – were also prepared. For each test duration, six columns were prepared for both test and control groups. The weights of the empty column, rubber stopper, vinyl hose, plastic mesh, and gauze were measured using an electronic balance prior to packing the soil and mixtures.

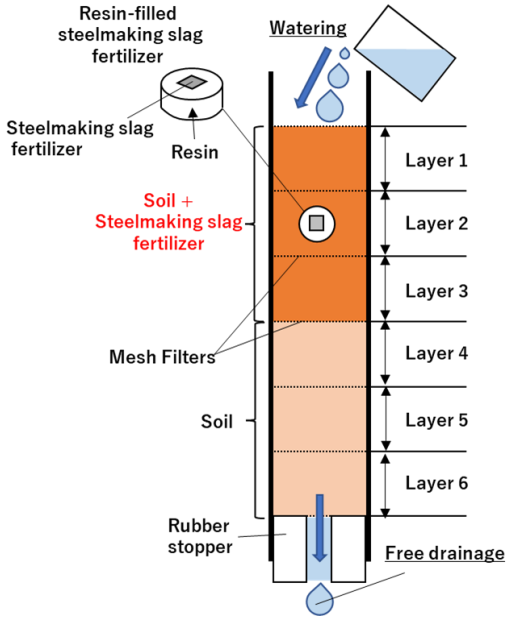

Fig. 2 Schematic of experimental apparatus.

2.3 Procedure

The experimental procedure is illustrated in Fig. 3. Each soil column containing a test sample was fixed inside an incubator maintained at 25 °C. A plastic container was placed below the vinyl hose at the bottom of the column to collect leachate. Then, 70 mL of distilled water was gently poured into the top of the column. The volume of distilled water was determined by dividing the average annual precipitation in Japan (Ministry of Land, Infrastructure, Transport and Tourism 2006) by the number of weeks in a year. After water infiltration was complete and leachate flow from the bottom ceased, a syringe equipped with a cartridge filter (pore size: 0.2 µm) was used to collect the leachate sample. The column was then kept inside the incubator for seven days. This cycle of water addition, leachate sampling, and incubation was repeated weekly for designated durations of 1, 2, 4, 8, 12, or 24 weeks. No water was added during the final week of each experiment. To determine the water content of the soil and soil–slag mixture samples within the columns, the total weight of each column and the amount of leachate collected were measured using an electronic balance before and after water addition. After completion of the leaching tests,

https://doi.org/10.5194/egusphere-2025-6356
Preprint. Discussion started: 30 December 2025

the columns were disassembled. The soil and soil–slag mixture layers, separated by plastic mesh, were collected layer by layer and air-dried in an incubator maintained at 40 °C for at least three days. The resin-embedded slag fertilizer samples were cleaned using an ultrasonic cleaner to remove any adhering soil and prepared for surface and cross-sectional observations.

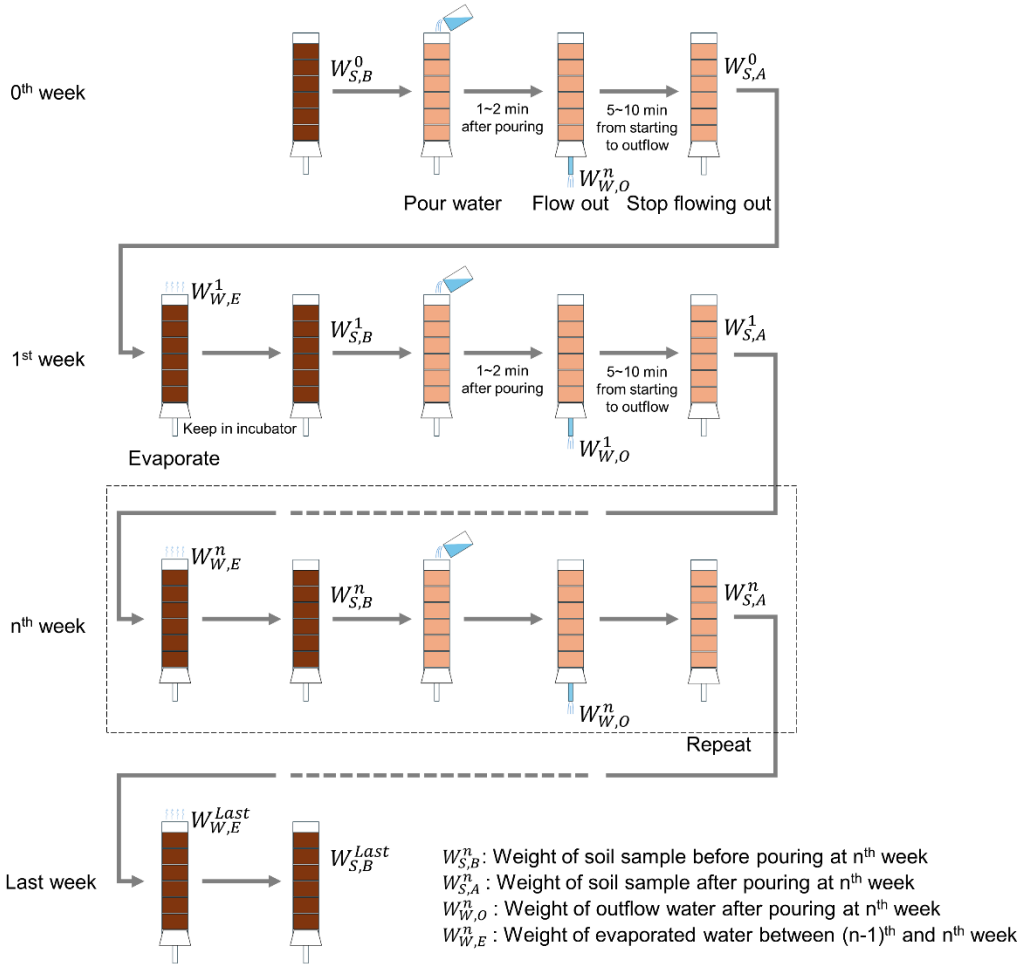

Fig. 3 Experimental procedure.

2.4 Analysis

After the experiments, the soil and soil–slag mixture samples were separated layer by layer and air-dried. The dried samples were then analyzed for soil pH, exchangeable cations, and plant-available phosphorus, based on standard methods for soil and crop nutrient diagnosis (Hokkaido Research Organization, Agricultural Research Department 2012). Soil pH was measured as follows: 20 g of the dried sample, sieved through a 2-millimeter mesh, was placed in a plastic bottle with 40 mL of distilled

https://doi.org/10.5194/egusphere-2025-6356
Preprint. Discussion started: 30 December 2025

water. After stirring for approximately 30 s and allowing the mixture to settle, a pH meter was inserted into the solution and the pH value was recorded after 30 s. For the analysis of exchangeable cations, 6 g of the dried sample, also sieved through a 2-millimeter mesh, was placed in a plastic bottle with 120 mL of 1N ammonium acetate solution (prepared by mixing 771 g of ammonium acetate with 9.4 L of distilled water). The mixture was shaken for 30 min using a horizontal shaker set to 160 rpm with a shaking amplitude of 40 mm. After extraction, the solution was filtered using a syringe equipped with a cartridge filter (pore size: 0.2 μm), and the concentrations of each element were measured by ICP–AES. To determine plant-available phosphorus, 3 g of the dried sample, sieved through a 0.5-millimeter mesh, was mixed with 600 mL of Truog's extractant (a solution prepared by mixing 30 g of ammonium sulfate, 20 mL of 1N sulfuric acid, and 9.98 L of distilled water) in a plastic bottle. The mixture was shaken under the same conditions for 30 min and the phosphorus concentration in the extract was measured using an atomic absorption spectrophotometer.

The resin-embedded slag fertilizer samples were mirror-polished prior to the leaching experiments and analyzed using an electron probe microanalyzer (EPMA) equipped with a wavelength-dispersive X-ray spectrometer to obtain elemental maps and conduct quantitative analysis. After the leaching tests, the resin-embedded samples were cleaned using an ultrasonic cleaner and air-dried, followed by additional EPMA analysis for elemental mapping and quantification. Finally, after surface analysis, each cylindrical resin-embedded sample was vertically cut, the cross-section was mirror-polished, and the same EPMA analyses were conducted on the polished cross-section.

3 Results

3.1 Temporal Changes in Soil pH and Exchangeable CaO and MgO

Figure 4 shows the soil pH, exchangeable cations, and plant-available phosphorus measurements for each soil layer at different leaching periods. In the control columns containing only soil, soil pH remains approximately 4.8 to 5.5 across all layers. In contrast, in the test columns, the pH of the first to third layers is higher (6.0 to 6.5) compared to the control, whereas the fourth to sixth layers, which contained only soil, show pH values similar to those in the control columns. Moreover, the elevated soil pH in the first to third layers of the test columns is maintained throughout the 24-week experimental period, indicating that the pH-increasing effect of the steelmaking slag fertilizer persists over time. No increase in soil pH is observed in the fourth to sixth layers of the test columns, where the slag fertilizer was not mixed.

https://doi.org/10.5194/egusphere-2025-6356
Preprint. Discussion started: 30 December 2025

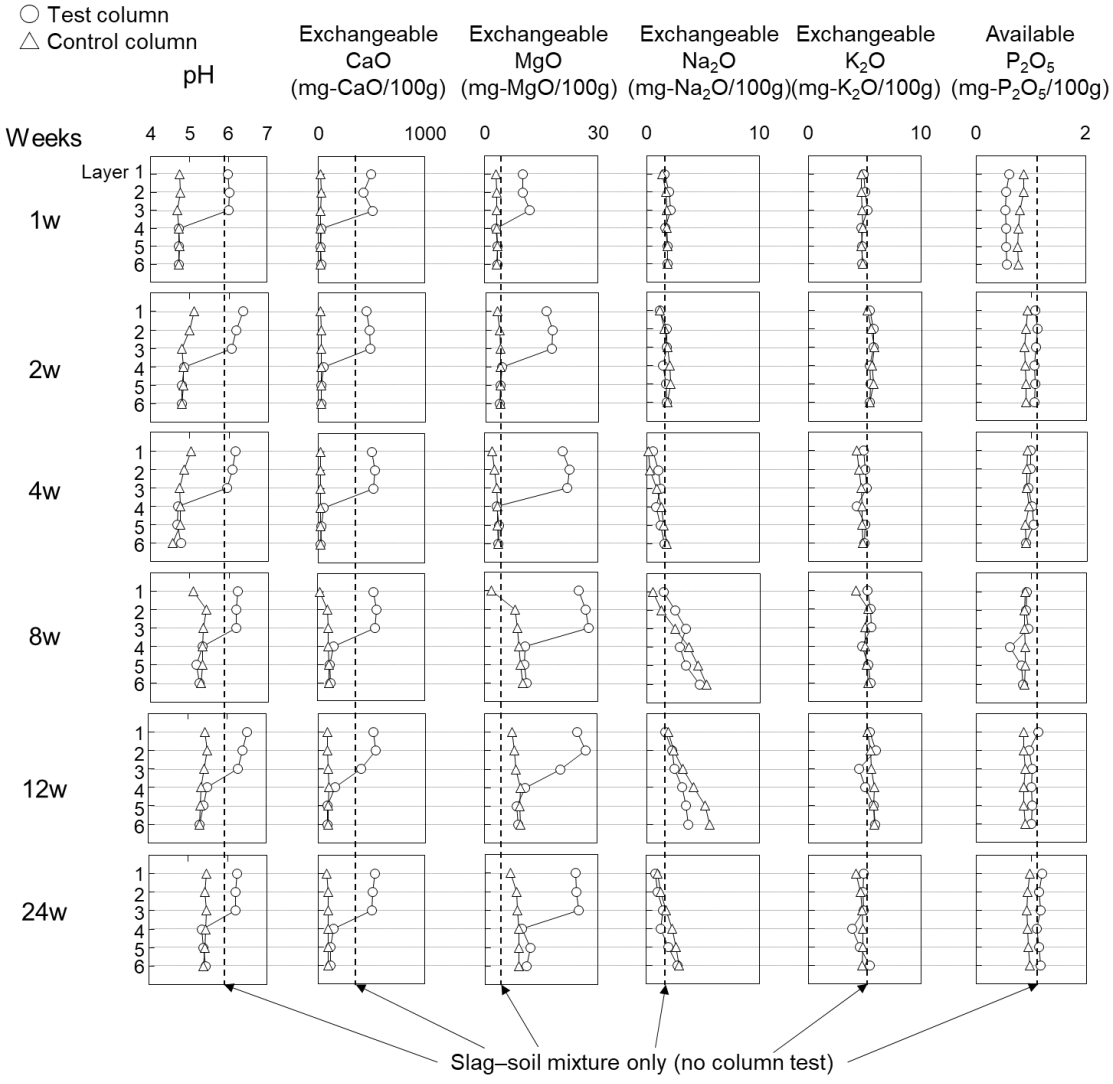

Fig. 4 Results of soil elution test.

Focusing on the changes in exchangeable CaO and MgO resulting from the application of steelmaking slag fertilizer, the test columns show an increase of approximately 400–500 mg per 100 g of dry soil in exchangeable CaO compared to the control, while the increase in exchangeable MgO is more modest, at approximately 10–30 mg per 100 g of dry soil. A similar trend as the soil pH is observed for exchangeable CaO and MgO, with elevated levels found only in the layers containing the soil–slag mixture. In contrast to calcium and magnesium, no increase in exchangeable Na_2O and K_2O is observed over time. For exchangeable Na_2O, both the test and control columns show a trend wherein the concentrations decrease in the upper layers and increase in the lower layers over time. With regard to plant-available phosphorus, the test columns show a slightly higher

https://doi.org/10.5194/egusphere-2025-6356
Preprint. Discussion started: 30 December 2025

trend throughout the leaching period. As shown in Table 1, the slag contains P_2O_5, and elevated levels are found not only in the upper three layers, where the soil–slag mixture was applied, but also in the lower three layers.

To compare the extent of leaching in the soil, a separate analysis was conducted using a sample in which soil and slag fertilizer were mixed but not subjected to the column leaching test; instead, the mixed sample was air-dried directly. The vertical dashed line in Fig. 4 represents the results from this control. In all cases (soil pH, exchangeable CaO, and MgO), the values are higher in the samples that underwent the column leaching test.

3.2 Surface of Slag Fertilizer Before and After Leaching

In the column leaching experiment, the same location on the surface of the resin-embedded slag fertilizer sample was observed before and after the test. Figure 5 shows secondary electron images, backscattered electron images, and elemental mapping of the resin-embedded sample before and after one week of the column leaching experiment. As the pre-experiment sample was polished, the phases constituting the slag can be clearly identified in the backscattered electron image and elemental mapping, as shown in Fig. 5(a). Table 2 presents EPMA values directly measured at points 1 to 4 in Fig. 5(a). Based on the elemental mapping, quantitative analysis, and the XRD pattern in Fig. 1, the mineral phases in this field of view include the C_2S phase with phosphorus solid solution; the MF phase composed of solid solutions of MgO, MnO, and FeO; the C_2F phase containing aluminum and titanium; and the f-CaO phase. In contrast to the flat surface of the pre-experiment sample, the surface after one week of leaching, as shown in Fig. 5(b), can be categorized into three major morphological types. The first type consists of precipitates formed in the central and upper-right areas of Fig. 5(b), which partially cover the surface of the original sample. The second type includes areas where the original surface is exposed but shows signs of cracking or surface roughening. The third type retains the original surface condition. Quantitative analysis at points 5 to 9 in Fig. 5(b) are shown in Table 2. Elemental mapping and the quantitative results indicate that the precipitates contain 5.3 mass% carbon, although only approximately 1 mass% was detected in the pre-experiment sample. The phases exhibiting cracking and surface roughening are primarily composed of calcium and silicon, or are rich in calcium, corresponding to the C_2S and f-CaO phases. After one week of leaching, these phases also showed the presence of carbon. The phases that maintain their original surface conditions are the MF phase, rich in magnesium and iron; and the C_2F phase, rich in calcium, iron, and aluminum. A small portion of the C_2S phase was also observed to retain its original surface state.

https://doi.org/10.5194/egusphere-2025-6356
Preprint. Discussion started: 30 December 2025

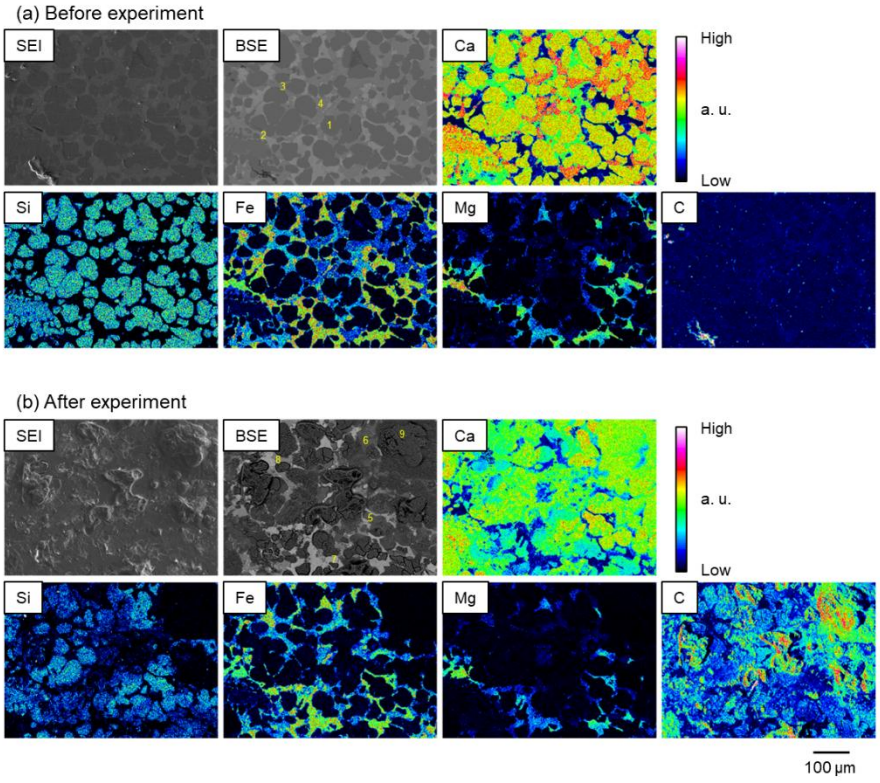

Fig. 5 Surface of slag (a) before and (b) after one week of embedment.

Table 2 Composition of phases before and after one week of leaching.

No.	Ca	Si	Fe	Mg	Al	P	Mn	Ti	C	O	Phase
1	40.4	11.8	0.7	0.0	0.4	3.0	0.0	0.2	1.2	30.2	C_2S
2	4.1	0.0	48.6	8.3	0.0	0.0	8.8	0.0	1.1	20.0	MF
3	29.1	0.6	23.1	0.3	5.4	0.1	0.5	4.0	1.1	25.0	C_2F
4	46.3	0.1	14.9	1.0	0.0	0.0	6.2	0.0	1.1	22.8	f-CaO
5	42.1	12.7	1.0	0.0	0.4	2.2	0.1	0.2	1.4	32.0	C_2S
6	42.1	11.8	0.8	0.0	0.4	2.0	0.1	0.1	4.8	35.8	C_2S (Altered phase)
7	4.8	0.1	51.7	7.5	0.0	0.0	7.9	0.0	0.9	21.5	MF
8	29.6	0.8	23.4	0.4	4.9	0.1	0.5	4.0	1.1	25.3	C_2F
9	32.3	0.1	0.2	0.0	0.0	0.0	0.1	0.0	5.3	22.1	$CaCO_3$

https://doi.org/10.5194/egusphere-2025-6356
Preprint. Discussion started: 30 December 2025

3.3 Time-lapse of Surface and Cross-section

To examine time-dependent changes in leaching behavior, representative results of surface observations after 1, 4, 8, and 24 weeks of leaching are shown in Fig. 6. As described earlier, after one week of leaching, the precipitates partially cover the sample surface, and the dissolution of the C_2S and f-CaO phases results in cracking. After four weeks, further dissolution of these phases produces visible pits, and a broader area of the surface is covered by precipitates. The MF and C_2F phases remain unchanged, as per the observation after one week. In the sample leached for eight weeks, cracking and pitting of the C_2S and f-CaO phases are still evident. In the sample leached for 24 weeks, precipitation occurred on the slag surface has progressed further, covering the entire surface of the precipitates.

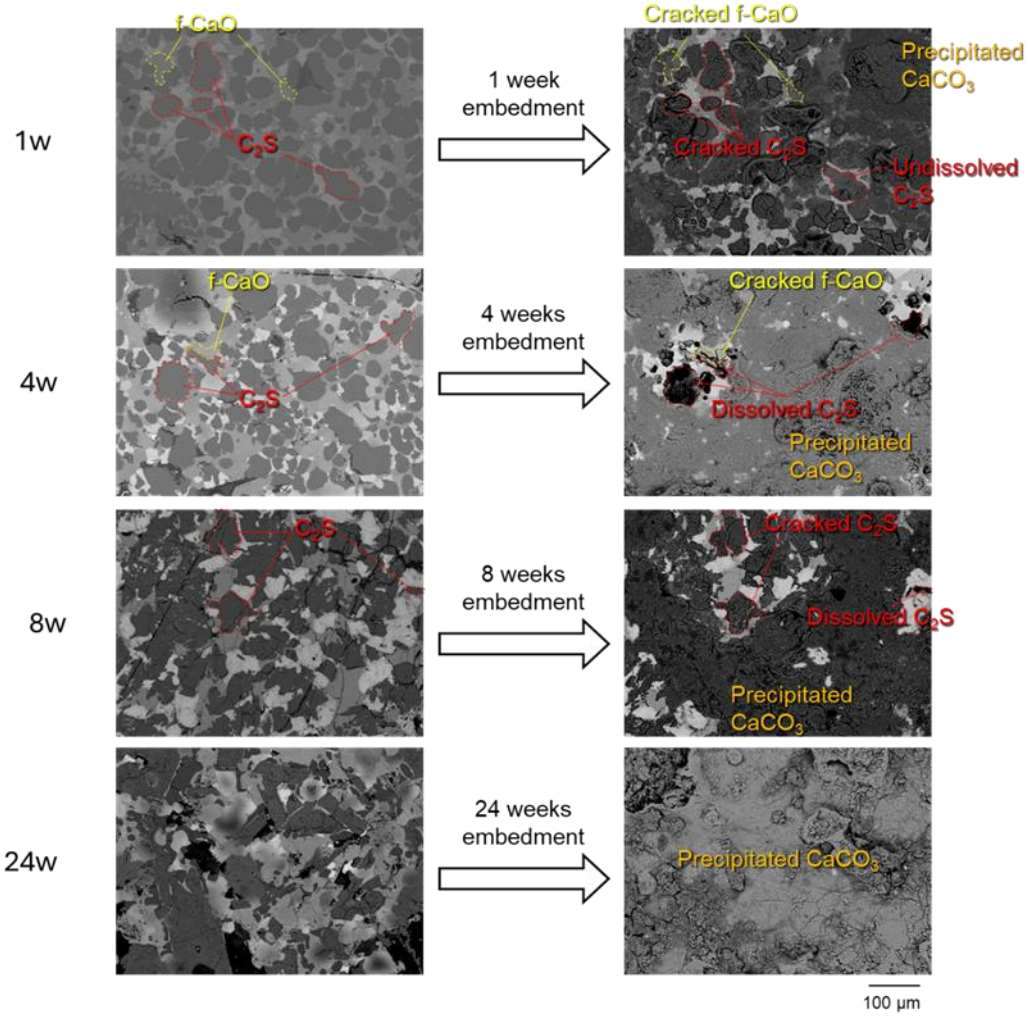

Fig. 6 Surface of slags before and after 1, 4, 8, and 24 weeks of embedment.

https://doi.org/10.5194/egusphere-2025-6356
Preprint. Discussion started: 30 December 2025

Cross-sections of the samples buried for 1, 12, and 24 weeks were cut and subjected to elemental mapping of calcium and carbon, as shown in Fig. 7. The precipitation on the original polished surface of the slag is also evident in Fig. 7. In the sample leached for one week, a layer with reduced calcium concentration extending inward from the slag surface was observed, with a maximum thickness of 31 μm and an average thickness of approximately 20 μm within the observed field. Moreover, the figure shows that leaching does not progress uniformly from the surface of the slag; rather, the extent of surface erosion varies by location, indicating non-uniform leaching. This is considered to be due to the preferential dissolution of the more soluble phases such as C_2S and f-CaO, as described previously. Even after extending the leaching period to 24 weeks, the depth of erosion remains nearly unchanged, with a maximum depth of 33 μm, and a similarly non-uniform leaching front is observed as in the one-week sample.

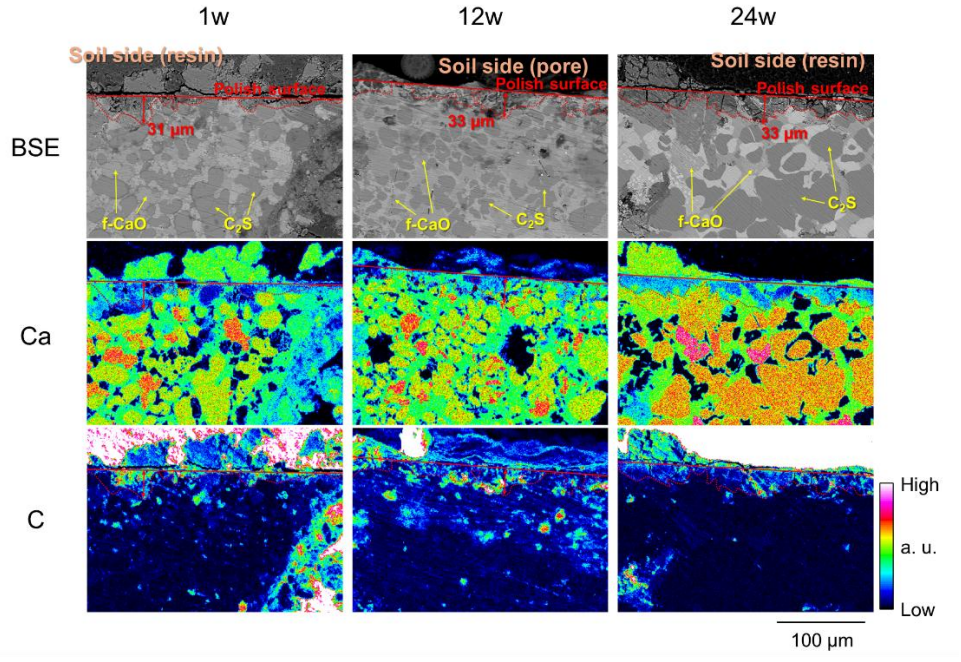

Fig. 7 Cross-section of embedded slag for 1, 12, and 24 weeks.

4 Discussion

4.1 Sources and Pathways of Ca Sustaining pH

Phases exhibiting cracking and surface roughening are primarily composed of calcium and silicon, or are rich in calcium, corresponding to the C_2S and f-CaO phases. In addition to cracking and roughening, surface alteration and pitting are observed on C_2S and f-CaO surfaces. After one week of leaching, precipitates containing measurable carbon are observed. Because the

https://doi.org/10.5194/egusphere-2025-6356
Preprint. Discussion started: 30 December 2025

concentrations of elements other than Ca and O are extremely low, these precipitates are identified as $CaCO_3$. Carbon is also detected in the altered phases formed on the surfaces of C_2S and f-CaO, which is consistent with dissolution in water followed by carbonation. Taken together, these observations indicate that the f-CaO and C_2S phases in the slag are the primary sources of calcium supplied to the soil, and that dissolution of these phases progresses over time and is accompanied by increasing precipitation of $CaCO_3$ on their surfaces.

The calculated solubility order shown below explains why calcium is released first from f-CaO and C_2S and subsequently retained as surface $CaCO_3$ that dissolves upon rewetting, sustaining elevated exchangeable CaO and pH.

According to previous reports (Gao et al. 2015; Futatsuka et al. 2004), the f-CaO phase and its reaction products $Ca(OH)_2$ and $CaCO_3$, as well as the C_2S phase are considered to leach into water according to Eqs. (1) to (4):

$$CaO(s) + 2H^+ = Ca^{2+} + H_2O \quad (1)$$

$$Ca(OH)_2(s) + 2H^+ = Ca^{2+} + 2H_2O \quad (2)$$

$$CaCO_3(s) + H^+ = Ca^{2+} + HCO_3^- \quad (3)$$

$$2CaO{\cdot}SiO_2(s) + 4H^+ = 2Ca^{2+} + H_2SiO_3 + H_2O \quad (4)$$

Figure 8 presents pH–solubility curves for the CaO, $Ca(OH)_2$, $CaCO_3$, and C_2S phases. In these calculations, the dissolution reactions of carbon dioxide (Eqs. (5) to (7)) and the dissociation reactions of the carbonate and metasilicate species (Eqs. (8) and (9)) were considered (Futatsuka et al. 2004). It was assumed that the CaO, $Ca(OH)_2$, and C_2S phases dissolved while maintaining the anion-to-cation ratios as defined by their chemical composition. For $CaCO_3$, solubility was calculated under various CO_2 partial pressures. The equilibrium constants for each reaction were calculated from the chemical potentials listed in Table 3 (Barin 1989; Chase 1998; Futatsuka et al. 2004; Pourbaix 1966; Pourbaix and Franklin 1974) using the Van't Hoff isotherm.

$$H_2O + CO_2(g) = H_2CO_3^0 \quad (5)$$

$$H_2CO_3^0 = H^+ + HCO_3^- \quad (6)$$

$$HCO_3^- = H^+ + CO_3^{2-} \quad (7)$$

$$H_2SiO_3^0 = H^+ + HSiO_3^- \quad (8)$$

$$HSiO_3^- = H^+ + SiO_3^{2-} \quad (9)$$

https://doi.org/10.5194/egusphere-2025-6356
Preprint. Discussion started: 30 December 2025

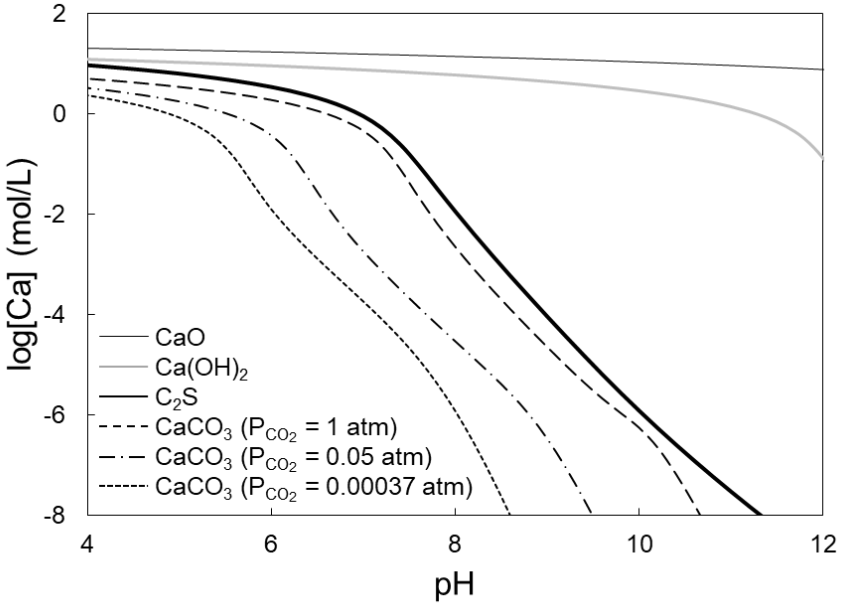

Fig. 8 pH–solubility curve for calcium compounds.

Table 3 Thermodynamic data for calculation of solubility.

Chemical species	State	μ°	Ref.
H^+	aq.	0	Pourbaix 1966
Ca^{2+}	aq.	-553,067	Pourbaix 1966
$H_2CO_3^0$	aq.	-624,445	Pourbaix 1966
HCO_3^-	aq.	-587,808	Pourbaix 1966
CO_3^{2-}	aq.	-528,129	Pourbaix 1966
$H_2SiO_3^0$	aq.	-1,012,512	Pourbaix 1966
$HSiO_3^-$	aq.	-955,053	Pourbaix 1966
SiO_3^{2-}	aq.	-887,050	Pourbaix 1966
H_2O	liq.	-237,141	Chase 1998
CO_2	gas	-394,389	Chase 1998
CaO	sol.	-603,592	Pourbaix and Franklin 1974
$Ca(OH)_2$	sol.	-898,421	Chase 1998
$2CaO{\cdot}SiO_2$	sol.	-2,198,590	Barin 1989
$CaCO_3$	sol.	-1,128,811	Barin 1989

https://doi.org/10.5194/egusphere-2025-6356
Preprint. Discussion started: 30 December 2025

The activity coefficient γ_i of chemical species i was calculated using Davies equation (Ritsema 1993):

$$\log \gamma_i = -0.509 z_i^2 \left(\frac{\sqrt{I}}{1+\sqrt{I}} - 0.31I\right) \quad (10)$$

$$I = \frac{1}{2}\sum_i C_i z_i^2 \quad (11)$$

where C_i and z_i are the concentration [mol/L] and charge of species i, respectively, and I is the ionic strength of the solution. From Fig. 8, it can be seen that within the soil pH range 4–7, and even at higher pH levels, phase solubility followed the sequence CaO > $Ca(OH)_2$ > C_2S > $CaCO_3$. Therefore, among these compounds, CaO, $Ca(OH)_2$, and the C_2S phase are readily leached, whereas $CaCO_3$ is relatively resistant to dissolution. The observed precipitates are considered to form as follows: First, Ca^{2+} ions are released from the f-CaO and C_2S phases, both of which exhibit high solubility. Since soil water is retained within soil pores, the areas near the dissolving phases experience an increase in both Ca^{2+} concentration and pH. At the elevated pH on the surface of the slag fertilizer, Ca^{2+} ions react with bicarbonate (HCO_3^-) and carbonate (CO_3^{2-}) ions formed from the dissolution of atmospheric CO_2 into water (Eqs. (12) to (15)), leading to the precipitation of $CaCO_3$.

$$CO_2(g) + H_2O = H^+ + HCO_3^- \quad (12)$$

$$Ca^{2+} + HCO_3^- = CaCO_3(s) + H^+ \quad (13)$$

$$CO_2(g) + H_2O = 2H^+ + CO_3^{2-} \quad (14)$$

$$Ca^{2+} + CO_3^{2-} = CaCO_3(s) \quad (15)$$

The cracking observed in the f-CaO and C_2S phases in this experiment is considered to be caused by their dissolution upon contact with water during infiltration, and by the volumetric expansion resulting from the formation of $Ca(OH)_2$ through the reaction of the f-CaO phase with water (Wang et al. 2010).

4.2 Ca^{2+} Supply and pH Enhancement under Column Leaching

To determine why pH and exchangeable cation levels were higher in the column samples than in those where soil and steelmaking slag fertilizer were simply mixed and dried, the following interpretation was made based on previous studies. According to a previous study in which mineral phases found in steelmaking slag were synthesized, pulverized to 53 μm or smaller, and subjected to leaching tests in a pH 5 nitric acid solution, the release of Ca^{2+} ions from C_2S continued even after 30 minutes (Gao et al. 2015). In the present study, slag fertilizer with a larger particle size was used, suggesting that the 30-minute shaking period used for the analysis of pH and exchangeable cations may not have been sufficient to complete the release of Ca^{2+} ions. Furthermore, the release of Ca^{2+} and Mg^{2+} ions from the slag promotes ion exchange with H^+ ions adsorbed

https://doi.org/10.5194/egusphere-2025-6356
Preprint. Discussion started: 30 December 2025

onto the soil surface, displacing them into the pore water. These H^+ ions are then either flushed out of the system by water infiltration or neutralized by OH^- ions generated during the slag dissolution process, which in turn increases the soil pH. Therefore, the observed increase in pH and exchangeable cation concentrations in the column samples is likely attributable to the extended reaction time within the column during the leaching period. On the other hand, previous studies (Gao et al. 2015; Iwama et al. 2020) have reported that the MF phase and the C_2F phase are resistant to leaching, which is consistent with the present observation that these phases maintain their original surface condition where exposed.

4.3 Agronomic Implications

Taken together with the solubility-based analysis, observations of slag surfaces and cross-sections suggest that the increase in soil pH reflects dissolution of alkaline components. In addition to the Ca^{2+} and Mg^{2+} that leach from the slag and become adsorbed onto soil particle surfaces, some of the extracted amounts likely originate from CaO and MgO contained in the slag fertilizer itself, as well as from precipitates formed during the leaching experiment. $CaCO^3$ is known to dissolve gradually in soil and provide a sustained increase in pH. Therefore, the long-term effectiveness of steelmaking slag fertilizer in improving soil pH may be attributed to its continuous supply of $CaCO_3$ to the soil. This precipitation of $CaCO_3$ helps retain calcium near the slag particles over an extended period, maintaining elevated levels of both soil pH and exchangeable CaO for at least 24 weeks. Both the downward movement of this fertilizer effect within the soil profile and runoff from upland fields are very small. This, in turn, suggests that the steelmaking slag fertilizer must be incorporated into the soil to the depth at which the effect is required to achieve soil pH improvement.

Since calcium and magnesium exhibit antagonistic interactions, where an excess of one can inhibit the uptake of the other, the desirable ratio of exchangeable CaO to exchangeable MgO in Japanese soils is considered to be approximately 65–75 : 20–25 in molar terms (Minister of Agriculture, Forestry and Fisheries 2008). Given that the observed increases are approximately 400–500 mg to 10–30 mg per 100 g of dry soil, the application of steelmaking slag fertilizer results in an excess of calcium. Therefore, it is advisable to apply a supplemental magnesium source depending on soil type and the crop being cultivated.

Since phosphate is generally immobile in soil, it is possible that contact with alkaline pore water alters the chemical form of phosphate, increasing its plant-availability.

4.4 Upland vs Paddy: Unique Carbonation

Although the dissolution of the C_2S phase has been previously observed in experiments simulating paddy field conditions (Ito 2022), precipitation of the $CaCO_3$ phase on the slag surface has not been reported.

In upland-type settings, repeated wetting and drying generate short periods of high pH and high Ca^{2+} concentration near dissolving slag particles. Aeration ensures a continuous CO_2 supply, while pore-scale water retention prolongs contact between porewater and reactive surfaces. These environmental conditions favor local supersaturation with respect to calcite, so thin

https://doi.org/10.5194/egusphere-2025-6356
Preprint. Discussion started: 30 December 2025

$CaCO_3$ skins form and thicken over time. By contrast, during continuous flooding, gas exchange is strongly suppressed and the supply of CO_2 to the soil solution is limited. Because wet–dry cycles are absent, supersaturation with respect to $CaCO_3$ is less likely and carbonate skins on slag surfaces are unlikely to form. This pattern appears to be characteristic of upland environments. From a management perspective, when long-term pH persistence via $CaCO_3$ cycling is desired, practices that allow intermittent drying and good aeration are advantageous. In continuously flooded systems, this mechanism is expected to weaken.

4.5 Mechanism of Slag Fertilizer Leaching in Soil

The leaching behavior of steelmaking slag fertilizer in soil under repeated wetting and drying conditions is inferred as illustrated in Fig. 9. First, infiltrating water reacts with and dissolves the C_2S and f-CaO phases. Simultaneously, water retained within the slag gradually penetrates these phases. The Ca^{2+} ions released through dissolution are partially transported away with migrating water, whereas the remaining Ca^{2+} ions within water retained in the soil react with the CO_3^{2-} ions formed by the dissolution and ionization of atmospheric CO_2, resulting in the formation of a $CaCO_3$ phase on the slag surface. Furthermore, CO_2 also dissolves into the water that has infiltrated the slag body, where it reacts with the C_2S and f-CaO phases to form altered phases. At the earliest stage, highly reactive f-CaO and C_2S phases are exposed in the slag, and cross-sectional observations suggest that the leaching depth is determined primarily by the initial slag–water reaction that occurs immediately after application. Subsequently, the newly infiltrated water dissolves both the previously precipitated $CaCO_3$ phase and the altered phase, thereby supplying further Ca^{2+}. This cycle of $CaCO_3$ precipitation and dissolution of both the altered and $CaCO_3$ phases is then repeated. Although the altered phase includes components that have reacted with CO_2, it mainly consists of the highly soluble C_2S and f-CaO phases, whose dissolution continues preferentially. As the leaching period is extended, this process manifests as the formation of pits. Because the $CaCO_3$ phase has lower solubility than the C_2S and f-CaO phases, Ca^{2+} released from these phases reacts with atmospheric CO_2 and precipitates as $CaCO_3$. Consequently, the surface coverage of $CaCO_3$ increases with prolonged leaching. Even after 24 weeks, a substantial amount of unreacted C_2S and f-CaO phases remain inside the particles, along with residual precipitated $CaCO_3$ on the surface. This indicates that the potential for calcium release from the slag remains well preserved at this stage.

https://doi.org/10.5194/egusphere-2025-6356
Preprint. Discussion started: 30 December 2025

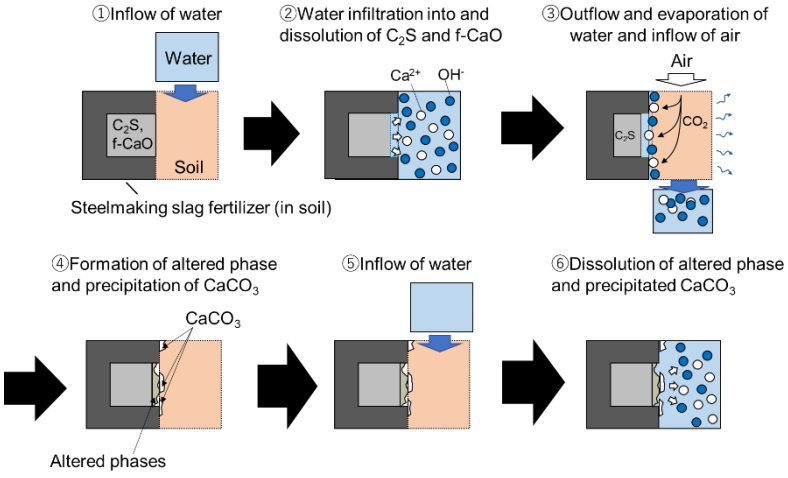

Fig. 9 Elution behavior of slag fertilizer in soil.

A similar mechanism can be considered for the leaching of Mg^{2+}. As MgO is contained in the f-CaO phase and is easily leached, it is likely to be released from the slag and migrate into the soil, where it reacts with atmospheric CO_2 to precipitate as $MgCO_3$. However, no distinct $MgCO_3$ phase was observed. This may be due to the greater supply of CaO than MgO from the slag. In addition, based on the phase compositions and leaching behaviors, it is likely that phosphate is supplied from the C_2S phase, and that the trace essential elements iron and manganese are supplied from the f-CaO phase.

5 Conclusion

To investigate the mechanisms of soil pH improvement and component leaching of slag fertilizer under upland conditions, a leaching test was conducted using a soil column system simulating an upland agricultural environment. The following conclusions are drawn from the results:

- In the control columns, soil pH remained approximately 4.8–5.5 throughout the experimental period. In contrast, in the test columns, the soil layers containing slag maintained a pH of 6.0–6.5, which remained stable without declining over the 24-week study period.
- Exchangeable CaO and MgO levels were higher in the slag-mixed layers of the test columns and were similarly maintained at elevated levels for 24 weeks.
- The f-CaO and C_2S phases contained in the slag were found to dissolve, and $CaCO_3$ precipitates formed on the slag surfaces. With longer leaching duration, the f-CaO and C_2S phases exhibited progressive dissolution, resulting in the formation of pits, while the surface coverage of $CaCO_3$ increased.
- Even after 24 weeks of leaching, the f-CaO and C_2S phases remained within the slag, and $CaCO_3$ deposits remained on the slag surface.

https://doi.org/10.5194/egusphere-2025-6356
Preprint. Discussion started: 30 December 2025

These findings demonstrate that fertilizer derived from steelmaking slag can provide sustained improvement in soil pH. The sustained release of calcium from the f-CaO and C_2S phases, along with the precipitation of $CaCO_3$, contributes to maintaining this effect over a period of at least 24 weeks. These results not only support the potential use of steelmaking slag fertilizer in upland agriculture but also suggest its added value and broader applicability as a recycled fertilizer material. In addition, this setup could be adapted, as needed, to quantify the partitioning of applied elements among the root-zone, subsoil, and outflow.

Data availability

The datasets generated and/or analyzed during the current study are available from the corresponding author on reasonable request.

Author contributions

Conceptualization: TI, SK, MO and SU. Data curation: TI and MO. Formal analysis: TI and SK. Investigation: TI and MO. Methodology: TI, SK and MO. Project administration: TI, SK and SU. Resources: SK and SU. Supervision: SU. Validation: TI, SK, MO and SU. Visualization: TI and SK. Writing (original draft preparation): TI and SK. Writing (review and editing): TI, SK, MO and SU.

Competing interests

The authors declare that they have no conflict of interest.

Financial support

The authors declare that no funds, grants, or other support were received during the preparation of this manuscript.

References

Ahire ML, Mundada PS, Nikam TD, Bapat VA, Penna S (2021) Multifaceted roles of silicon in mitigating environmental stresses in plants. Plant Physiol Biochem 169:291–310. https://doi.org/10.1016/j.plaphy.2021.11.010

https://doi.org/10.5194/egusphere-2025-6356
Preprint. Discussion started: 30 December 2025

Appelo CAJ, Postma D (2004) Geochemistry, Groundwater and Pollution. 2nd edn. CRC Press, London.

Barin I (1989) Thermochemical data of pure substances. VCH, New York, (1989).

Chase MW (ed) (1998) NIST-JANAF Thermochemical Tables. 4th edn. J Phys Chem Ref Data, Monograph 9. American Institute of Physics.

595 Deus ACF, Büll LT, Guppy CN, Santos SMC, Moreira LQM (2020) Effects of lime and steel slag application on soil fertility and soybean yield under a no til-system. Soil Tillage Res 196:104422. https://doi.org/10.1016/j.still.2019.104422

Food and Agriculture Materials Inspection Center (2024) To establish official standards for ordinary fertilizers in accordance with the Law Concerning Assurance of Fertilizer Quality, etc (in Japanese).
600 http://www.famic.go.jp/ffis/fert/kokuji/60k0284.pdf Accessed 5 Sep 2025

Furuzono S, Hidaka H, Yamashita K (2022) A Simplified Method for Evaluating Available Silica in Siliceous Materials Using the Reciprocating Shake Extraction Method with Neutral Tris Buffer (in Japanese). Nippon Dojo-Hiryogaku Zassh 93:392–397. https://doi.org/10.20710/dojo.93.6_392

Futatsuka T, Shitogiden K, Miki T, Nagasaka T, Hino M (2004) Dissolution Behavior of Nutrition Elements from
605 Steelmaking Slag into Seawater. ISIJ Int 44:753–761. https://doi.org/10.2355/isijinternational.44.753

Gao X, Maruoka N, Kim SJ, Ueda S, Kitamura S (2015) Dissolution Behavior of Nutrient Elements from Fertilizer Made of Steelmaking Slag, in an Irrigated Paddy Field Environment. J Sustain Metall 1:304–313. https://doi.org/10.1007/s40831-015-0030-8

Goto I (2016) Development and Promotion of Agricultural Utilization Technology for Converter Slag (in Japanese).
610 Shokubutsu-Boeki (Plant Prot) 70:209–214. https://jppa.or.jp/archive/pdf/70_04_01.pdf Accessed 5 Sep 2025

Gu WF, Diao J, Tao HR, Deng JY, Yu HY, Iwama T, Ceremisina E, Li HY, Xie B, Ueda S (2025) Effects of Cooling Methods on Phase Evolution, Microstructure, and Stability of Steelmaking Slag. Metall Mater Trans B 56:3970–3979. https://doi.org/10.1007/s11663-025-03618-4

Hokkaido Research Organization, Agricultural Research Department (2012) Analytical Methods for Soil and Crop
615 Nutrition Diagnostics 2012 (in Japanese). https://www.hro.or.jp/upload/13651/0.pdf Accessed 5 Sep 2025

Inubushi K (2021) Sustainable soil management in East, South and Southeast Asia. Soil Sci Plant Nutr 67:1–9. https://doi.org/10.1080/00380768.2020.1835431

Inubushi K, Saito H, Arai H, Ito K, Endoh K, Yashima MM (2018) Effect of oxidizing and reducing agents in soil on methane production in Southeast Asian paddies. Soil Sci Plant Nutr 64:84–89.
620 https://doi.org/10.1080/00380768.2017.1401907

Ito K (2015) Suppression of Methane Gas Emission from Paddy Fields. Nippon Steel and Sumitomo Metal Tech Rep 109:145–148. https://www.nipponsteel.com/en/tech/report/nssmc/pdf/109-25.pdf Accessed 5 Sep 2025

https://doi.org/10.5194/egusphere-2025-6356
Preprint. Discussion started: 30 December 2025

Ito K (2022) Elution of Plant Nutrition Elements from Steel Slag Fertilizers in a Paddy Field. Nippon Steel Tech Rep 127:100–108, 100. https://www.nipponsteel.com/en/tech/report/pdf/127-17.pdf Accessed 5 Sep 2025

Ito K, Endoh K, Shiratori Y, Inubushi K (2015) Silicon elution from three types of steel slag fertilizers in a paddy field analyzed by electron probe micro-analyzer (EPMA). Soil Sci Plant Nutr 61:835–845. https://doi.org/10.1080/00380768.2015.1064326

Iwadate Y (2017) Reducing Soil-Borne Disease Damage Through Soil pH Improvement Using Converter Slag (in Japanese). Tsuchidukuri-to-Ekonogyo 49:42–47. https://cir.nii.ac.jp/crid/1522262180006849280 Accessed 5 Sep 2025

Iwama T, Du CM, Koizumi S, Gao X, Ueda S, Kitamura SY (2020) Extraction of Phosphorus and Recovery of Phosphate from Steelmaking Slag by Selective Leaching. ISIJ Int 60:400–407. https://doi.org/10.2355/isijinternational.ISIJINT-2019-298

JOGMEC (2021) Mineral Resources Material Flow, 2021, 27. Phosphorus (in Japanese). https://mric.jogmec.go.jp/wp-content/uploads/2023/03/material_flow2021_P.pdf Accessed 5 Sep 2025

Li G, Liu P, Chao S, Zhang X, Li J, Zhang Y, Duan Y (2024) The mineral phase evolution characteristics and hydration activity enhancement mechanism of steel slag under NaOH alkaline excitation. J Alloys Compd 978:173524. https://doi.org/10.1016/j.jallcom.2024.173524

Maruoka N, Okubo M, Shibata H, Gao X, Ito T, Kitamura S (2015) Improvement of Desalted Paddy Soil by the Application of Fertilizer Made of Steelmaking Slag (Recovery of a Paddy Field Damaged by the Tsunami Using Fertilizer Made of Steelmaking Slag-1) (in Japanese). Tetsu-to-Hagané 101: 445–456. https://doi.org/10.2355/tetsutohagane.TETSU-2014-131

Matsubae-Yokoyama K, Kubo H, Nakajima K, Nagasaka T (2009) A Material Flow Analysis of Phosphorus in Japan. J Ind Ecol 13:687–705. https://doi.org/10.1111/j.1530-9290.2009.00162.x

Matsui S (2020) Stabilization of Calcium Compounds in Steelmaking Slag. Nippon Steel Tech Rep 125:93–98. https://www.nipponsteel.com/en/tech/report/pdf/125-17.pdf Accessed 5 Sep 2025

Minister of Agriculture, Forestry and Fisheries (2008) Publication of Basic Guidelines for Geo-Enhancement (in Japanese). https://www.maff.go.jp/j/seisan/kankyo/hozen_type/h_dozyo/pdf/chi4.pdf Accessed 5 Sep 2025

Ministry of Land, Infrastructure, Transport and Tourism (2006) Rivers in Japan. https://www.mlit.go.jp/river/basic_info/english/pdf/riversinjapan.pdf Accessed 5 Sep 2025

Murakami K, Goto I (2006) Control of Clubroot Disease in Brassica Vegetables through High Application of Converter Slag (in Japanese). Agric Hortic 81:445–452. https://agriknowledge.affrc.go.jp/RN/2010723613.pdf Accessed 5 Sep 2025

https://doi.org/10.5194/egusphere-2025-6356
Preprint. Discussion started: 30 December 2025

National Agriculture and Food Research Organization (2015) Damage Reduction Techniques for Soilborne Fusarium Disease by Correcting Soil pH with Converted Slag as a Core Technology, Research Results (in Japanese). https://www.naro.go.jp/publicity_report/publication/archive/files/tenro-slag-2.pdf Accessed 5 Sep 2025

Nippon Slag Association (2015) Characteristics and Usefulness of Steel Slag Products (in Japanese). https://www.slg.jp/cms/wp-content/themes/original/pdf/pamph-sustainability_2015.pdf Accessed 5 Sep 2025

Nippon Slag Association (2024) Overview of steel slag supply and demand in FY2023 (in Japanese). https://www.slg.jp/cms/wp-content/themes/original/pdf/slag-overview_2023.pdf Accessed 5 Sep 2025

Okubo M, Maruoka N, Shibata H, Gao X, Ito T, Kitamura S (2015) Long-term Dissolution Characteristics of Various Fertilizers Made of Steelmaking Slag in a Desalted Paddy Soil Environment (Recovery of a Paddy Field Damaged by the Tsunami Using Fertilizer Made of Steelmaking Slag-2) (in Japanese). Tetsu-to-Hagané 101:457–464. https://doi.org/10.2355/tetsutohagane.TETSU-2014-132

Pourbaix M (1966) Atlas of Electrochemical Equilibria. Pergamon Press, Oxford.

Pourbaix M, Franklin JA (1974) Atlas of electrochemical equilibria in aqueous solutions, 2nd ed. National Association of Corrosion Engineers, Houston.

Ritsema CJ (1993) Estimation of activity coefficients of individual ions in solutions with ionic strengths up to 0.3 mol dm^{-3}. Eur J Soil Sci 44:307–315. https://doi.org/10.1111/j.1365-2389.1993.tb00454.x

Saigusa M, Matsuyama N (1998) Distribution of allophanic andosols and non-allophanic andosols in Japan. Tohoku J Agricul Res, 48:75–83. https://ci.nii.ac.jp/naid/110000982233 Accessed 5 Sep 2025

Shiratori Y (2024) Development of Methane Emission Control Measures for Rice Paddy Fields and Visualization Technology for Hydrogen Sulfide (in Japanese). Hiryo-Kagaku (Fert Sci) 46:73–97. https://www.jstage.jst.go.jp/article/fertilizerscience/46/0/46_73/_pdf/-char/ja Accessed 5 Sep 2025

Sinegovskaya VT, Banetskaya EV, Boiarskii BS, Sinegovskii MO, Nikulchev KA (2020) Role of soil liming in increasing crop yields in crop rotation. IOP Conf Ser: Earth Environ Sci 547:012037. https://doi.org/10.1088/1755-1315/547/1/012037

Verma KK, Song XP, Liang Q, Huang HR, Bhatt R, Xu L, Chen GL, Li YR (2024) Unlocking the role of silicon against biotic stress in plants. Front Plant Sci 15:1430804. https://doi.org/10.3389/fpls.2024.1430804

Wang G, Wang Y, Gao Z (2010) Use of steel slag as a granular material: Volume expansion prediction and usability criteria. J Hazard Mater 184:555–560. https://doi.org/10.1016/j.jhazmat.2010.08.071

Yamamoto S, Morii H (2020) Suppression of Methane Production via the Promotion of Fe^{2+} Oxidation in Paddy Fields. Commun Soil Sci Plant Anal 51:1114–1122. https://doi.org/10.1080/00103624.2020.1751192